Journal of Climate Change Action, 2024, Vol. X, Iss. X, 1-11

DOI: 10.62184/jcca.jccaj100020241

Research Article

SCIENCE PARK PUBLISHER

Journal of Climate Change Action

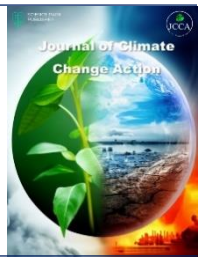

Electrospun Nylon 6 Nanofibers for Oil/Water Separation

Faten Riad[1], Hesham Ibrahim[1], Moataz Soliman[2], Shaker Ebrahim[2], Azza Shokry[2,*]

[1] Department of Environmental Studies, Institute of Graduate Studies and Research, Alexandria University, P.O. Box 832, Alexandria, Egypt

[2] Department of Materials Science, Institute of Graduate Studies and Research, Alexandria University, P.O. Box 832, Alexandria, Egypt

Received: 05, 01, 2024; Accepted: 14, 07, 2024; Published: 27, 07, 2024

Abstract

Oil-water separation is a difficult process, and many reported materials have the drawbacks of low oil absorption which limit their application. Herein, we reported nylon 6 nanofibers prepared by the electrospinning process using formic acid. The nanofibers' surface morphology, crystallinity, hydrophobicity, and sorption capacity were studied. Morphological analysis of 30 wt % nylon 6 /formic acid demonstrated uniform nanofibers that are free from beads with an average diameter varying from 30 to 90 nm. The results revealed that the contact angle of nylon 6 nanofibers is observed as 61º which refers to the nanofibers being slightly hydrophilic. The optimal preparation process was determined by 30 wt % nylon 6 /formic acid concentration, a flow rate of 0.5 ml/hr, an applied voltage of 15 kV, an immersion time of 30 min and the oil absorption capacity was 85.38 g/g. The sorption capacity of nylon 6 nanofibers is higher than some other reported adsorbents making it a promising material for water purification.

Keywords: Nylon 6, Electrospinning, Nanofibers, Oil spill, Removal

1. Introduction

Oil is a class of pollutants with very low affinity to water. The thinnest layer of oil can affect the aquatic environment by decreasing both the penetration of light and the oxygen transfer between air and water leading to the death and deterioration of the aquatic organisms. Therefore, discharge limits for oil and grease are imposed by environmental law [1]. Current methods of controlling oil spills include chemical treatment [2], physical adsorption [3], skimming [4], using booms [5], and burning the oil on the surface of the water [6].

Among these different techniques, physical adsorption is considered to be an efficient and economical cleaning method in oil pollution treatment due to its easy manufacture, low production cost, environmental friendliness, high selectivity, and recyclability [7].Up to now, polymeric nanofibers have been used as oil absorbents due to their unique physical and mechanical properties, high surface area, and small pore sizes [7, 8] expelling water due to their hydrophobic and oleophilic characteristics [9-11]. There are different techniques have been used to fabricate polymeric nanofibers such as template synthesis [12], phase separation [13], drawing [14], and electrospinning [15]. The electrospinning method is used to produce continuous fine nanofibers with inner diameters of 10 μm down to 10 nm by allowing a polymer solution or melts with an electrical driving force [16, 17]. The advantages of this technique are the low cost, relative easiness, and high versatility by controlling the fiber diameter [18].

In the present work, we reported the fabrication of nylon 6 nanofibers through a low-cost and simple process by electrospinning technique for the adsorption of motor oil. The

DOI: 10.62184/jcca.jccaj100020241

Research Article

effects of different electrospinning parameters on the morphology of the nanofibers are studied. These nanofibers are morphologically and structurally characterized. The hydrophilicity and the oil sorption capacities of the prepared nylon 6 sorbent for motor oil are evaluated.

2. Experimental

2.1. Materials

Nylon 6 granules grade of Tecomid NB40 NLE with a density of 1.13 g/ cm^3 was obtained from Eurotec company (Turkey), formic acid (85%) with analytical grade was purchased from Elgomhoreya chemical company (Egypt), motor oil 600/700 with a density of 0.8825 g/ cm^3 according to American Society for Testing and Materials (ASTM) 4052 and molecular weight 550 g/mol according to ASTM 2502 composed of hydrocarbons chain (-C40-) was obtained from Amoc company, Alexandria (Egypt).

2.2. Preparation of nylon 6 nanofiber

Electrospinning technique employed to synthesize the nylon6 nanofiber by means of a laboratory-scale electrospinning device. The device consists of 30 kV DC power supply (Hipotronics), a syringe pump (New Era Pump Systems, Inc., NY, USA) with a conducting tip needle, spinneret, and collector plate grounded and separated from the spinneret by a defined distance. The nylon6 solution containing different amounts of nylon6/formic acid (10,20 and 30 wt%) was then electrospun using the syringe pump with a 0.5 mm diameter needle tip at a feeding rate varied from 0.2 to 1ml/hr. The applied working voltage using the DC high voltage power supply (DC-PS) varied from 5 to 20 kV, as explained later. The distance between the syringe (spinneret) tip and the collector plate was 5 cm. The collector plate was grounded and covered by aluminum foil, and the syringe needle was fastened to the positive electrode of the DC-PS before use.

2.3. Characterization of nylon 6 nanofiber

The chemical interactions and surface modification of nylon 6 nanofiber were confirmed by Fourier-transform infrared (FTIR) spectroscopy (Spectrum BX 11- LX 18–5255 Perkin Elmer). The spectra were recorded in the spectral range from 4,000 to 500 cm^{-1}. The morphologies of the electrospun nanocomposites were assessed by scanning electron microscope (SEM) (Joel JSM 5300, Japan). The crystalline structure was evaluated by X-ray 7000 Shimadzu-Japan. The contact angle of water droplets was measured on the Rame-Hart contact angle goniometer (Rame-Hart Instrument Company, France).

2.4. Oil sorption experiments

Nylon 6 nanofibers obtained by electrospinning technique at various preparation conditions were tested for their performance in the sorption of crude oil spills. The nanofibers were cut into square pieces, dried at 70 C^o for 1 hr, vacuumed for 2 hrs, and weighed. The samples were then immersed in 10 mL of motor oil. After various time intervals of up to 30 min, the mass of each sample was measured as a function of time [19]. The oil sorption capacity (Q, g/g) was calculated as follows [20]:

$$Q = \frac{m_s - m_0}{m_0} \quad (1)$$

where m_s is the total mass of the sorbent after the oil adsorbed and m_0 is the mass of the dry sorbent.

3. Results and discussion

3.1. Structural analysis

FTIR spectra of nylon 6 and nylon 6 nanofiber are displayed in Figure 1 (a and b). The main characteristic bands of nylon 6 (Figure 1a) observed at 3304, 2856, 2940, 1646, 1544, 690, and 578 cm^{-1} are assigned to N-H stretching, CH_2 stretching, CH_2 stretching, amide I stretching, amide II due to carbonyl stretching, C-C bending and C-C deformation respectively [21, 22]. Nylon 6 nanofiber shown in Figure 1b has similar bands of nylon 6 film, the transmittance bands observed at 2374 and 1746 cm^{-1} correspond to O-H and C=O refers to formic acid groups [23].

Journal of Climate Change Action, 2024, Vol. X, Iss. X, 1-11

DOI: 10.62184/jcca.jccaj100020241

Research Article

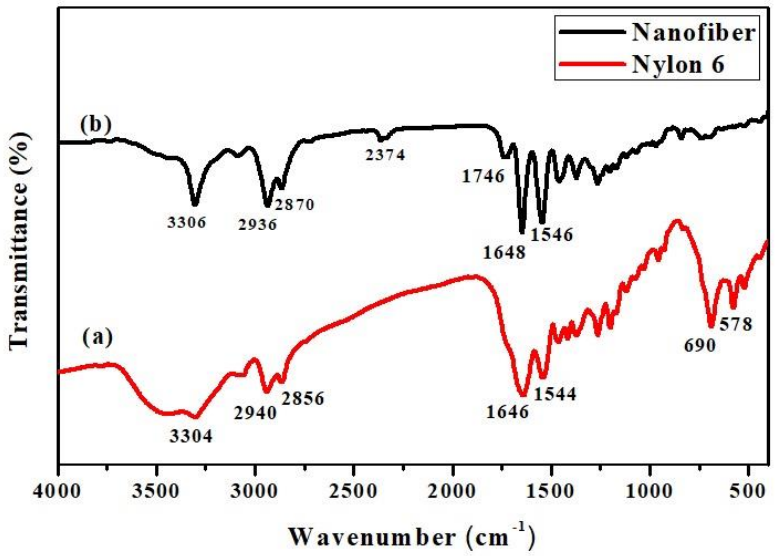

Figure 1. FTIR spectra of (a) nylon 6 and (b) nylon 6 nanofiber.

The crystalline structure of nylon 6 powder and nanofiber are shown in Figure 2 (a and b). The XRD pattern of nylon 6 film (Figure 2a) exhibits two sharp peaks at 2θ=20.5º and 2θ = 24.5º corresponding to the characteristic of the α- phase. By calculating the crystal size from the Scherrer equation, the crystal size is 3.425 nm. However, the diffraction pattern of nylon 6 nanofiber (Figure 2b) displays two smaller peaks at 2θ =20.3º and 2θ = 23.6º. The formation of small and/or defective crystals is due to the rapid vaporization of the solvent during the electrospinning process which does not allow sufficient time for the ordering of the molecules [24]. Electrospinning could also result in the formation of γ-crystalline structure for nylon 6, where the formation of γ -crystalline structures requires a rapid crystallization rate and this suggests that nylon 6 crystallization was rapid [25].

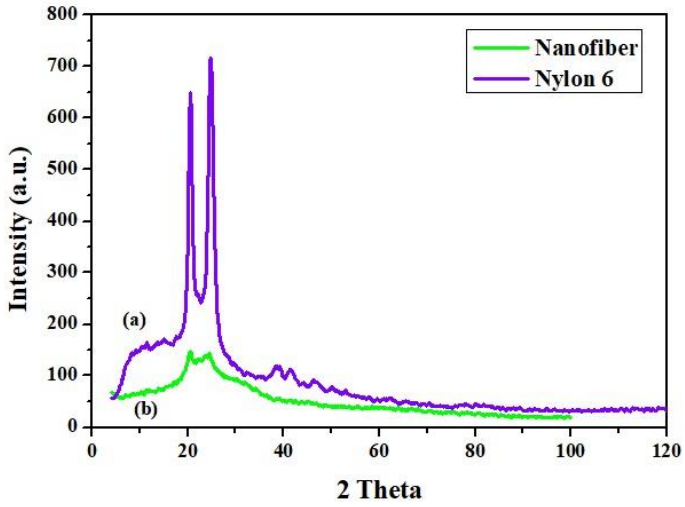

Figure 2. XRD patterns of (a) nylon 6 and (b) nylon 6 nanofiber.

DOI: 10.62184/jcca.jccaj100020241

Research Article

3.2. Morphological analysis of nylon 6 nanofiber at different conditions

3.2.1. Effect of solution concentration

The SEM micrographs of nylon 6 nanofibers made of different concentrations of nylon 6/ formic acid wt % solutions and their diameter range distributions are presented in Figure 3. It is observed that the solution of 10 wt % did not produce nanofibers. Rather the electrospraying occurs as shown in Figure 3a with the production of beads or droplets falling on the collector target. This was reported owing to the low viscosity and high surface tensions of the solution. When an electric field is applied to any droplet, the electric charge generates an electrostatic force inside the droplet, known as the Coulomb force, which competes with the cohesive force intrinsic to the droplet [26]. When the applied Coulomb force can overcome the cohesive force of the droplet manifested in the surface tension, the droplet will undergo break up into smaller droplets in the micro- to nano-scales. This phenomenon begins at the Taylor Cone, referring to the progressive shrinkage of the unstable, charged macro-droplet into a cone from which the smaller charged droplets will be ejected as soon as the surface tension is overcome by the Coulomb force [27].

At 20 wt% nylon 6 solution (Figure 3b), the amount of the fiber increases but still contains a lot of beads. The nanofibers produced are associated with beads due to the instability of the jet under different process conditions. Beads are expected to form at times during electrospinning whenever the surface tension forces tend to overcome the forces (such as charge repulsion and viscoelastic forces) that favor the elongation of a continuous jet. This is consistent with the observation that electrospinning dilute solutions of polymers, where chain entanglement is limited, tend to result in bead formation. With the polymer solutions electrospun at a fixed electric field, some beading is invariably obtained in the critical concentration regime where the transition from electrospraying of droplets into electrospinning occurs. This is related to incipient chain entanglement gradually overcoming the surface tension forces at higher polymer concentrations.

On the other hand, at 30 wt % nylon 6 solutions, the nanofibers formed were free from the beads which formed as a thin layer as shown in Figure 3c. Thirty measurements were conducted to analyze the average diameter for using software Digimizer. A trace of fibers produced from nylon 6 nanofiber from 10 wt % in the range from 10 to 30 nm (Figure 3d). For a concentration of 20 wt % solution, the average diameters are in the range from 10 to 60 nm and the dominant diameter is in range of 30 to 40 nm (Figure 3e). The average fiber diameter of the nylon 6 nanofiber electrospun from 30 wt % solutions is much bigger than from a 20 wt % solution, as it is ranged from 30 to 90 nm, and the dominant diameter, is in range of 40 to 50 nm (Figure 3f).

When the concentration is suitable, smooth homogeneous sheet nanofibers can be obtained [28]. For a concentration of 40 wt % nylon 6, the solution was dried very quickly when exposed to air due to the evaporation of formic acid which leads to the clogging of the syringe and prevents pumping. Consequently, the 30 wt % solution is considered the optimum concentration for the electrospinning of nylon 6.

Figure 4 (a and b) show two photographs of nanofibers formed from electrospray of 10 and 30 wt % of nylon 6, respectively.

Journal of Climate Change Action, 2024, Vol. X, Iss. X, 1-11

DOI: 10.62184/jcca.jccaj100020241

Research Article

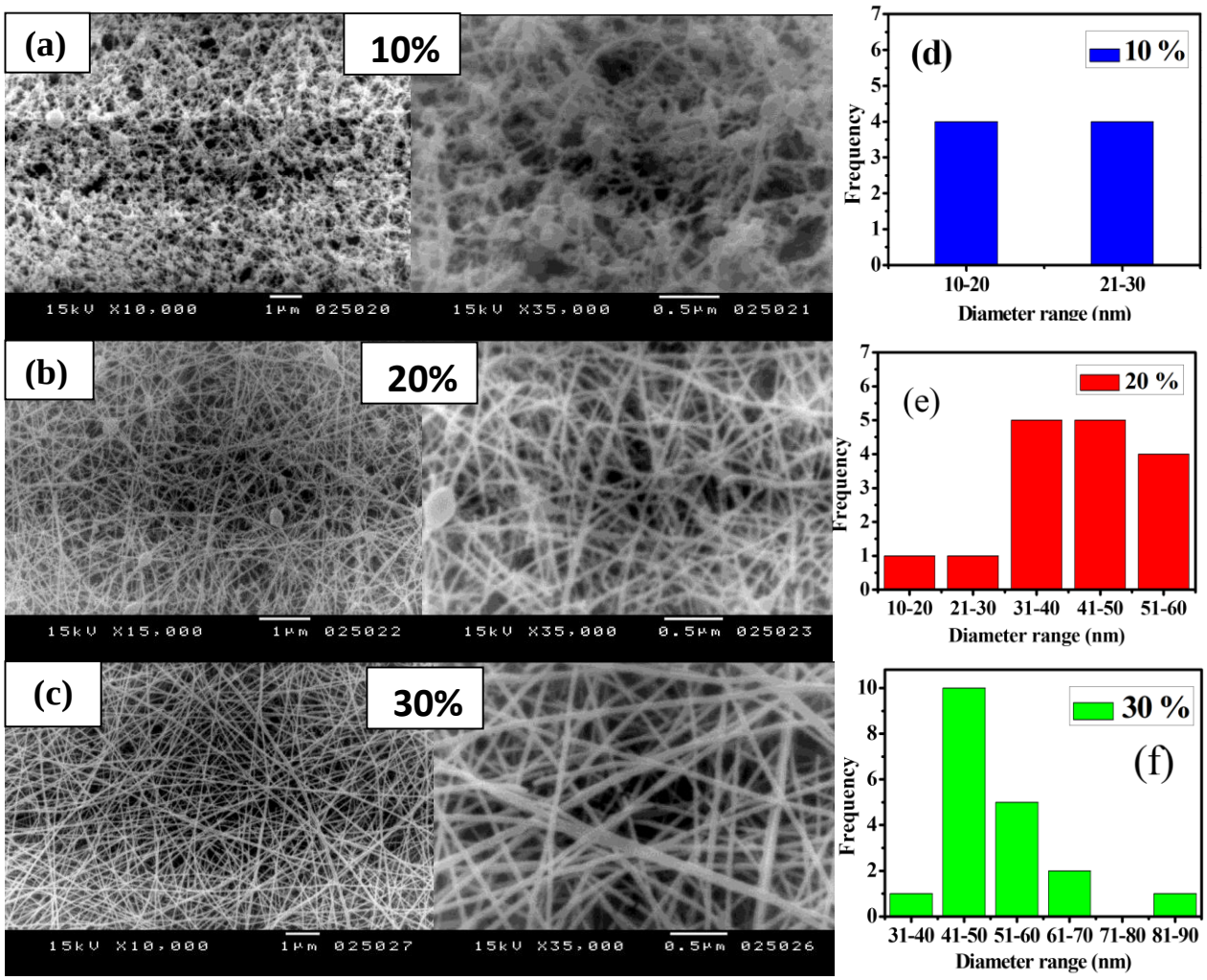

Figure 3. SEM micrographs of (a) the beaded structures obtained at concentration of 10 wt% (b) the nonbeaded structures obtained at 20 wt % and (c) 30 wt %, and nanofiber diameter range distribution from SEM images of structures obtained at concentration of (d) 10 wt %, (e) 20 wt % and (f) 30 wt % of nylon 6 nanofibers at constant applied voltage of 15 kV.

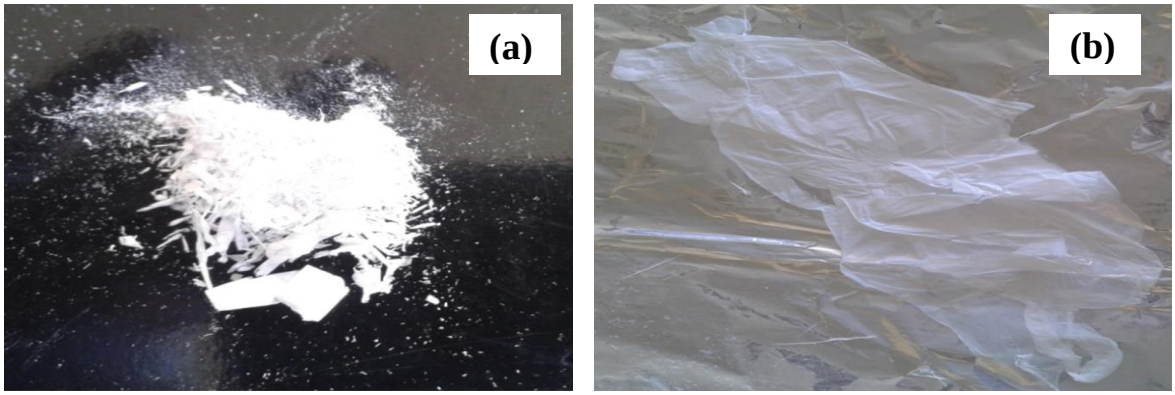

Figure 4. Photographs of nanofibers formed from electrospray of (a) 10 wt % and (b) 30 wt % of nylon 6.

Journal of Climate Change Action, 2024, Vol. X, Iss. X, 1-11
DOI: 10.62184/jcca.jccaj100020241

Research Article

3.2.2. Effect of the applied voltage

Maintaining a fixed nylon 6/formic acid concentration of 30 wt % and fixed spinneret tip-to-collector distance at 5 cm, the electrospinning applied voltage was varied from 5 to 20 kV (5, 10, 15 and 20 kV). In order for the electrospinning jet to get powered, a critical voltage must be achieved. The high voltage will induce the necessary charges on the solution will initiate the electrospinning process when the electrostatic force in the solution overcomes the surface tension of the solution [31]. Generally, both high negative or positive voltage of more than 5kV is able to cause the solution drop at the tip of the needle to distort into the shape of a Taylor Cone during jet initiation. Depending on the feed rate of the solution, a higher voltage may be required so that the Taylor Cone is stable. The Coulomb repulsive force in the jet will then stretch the viscoelastic solution [32]. If the applied voltage is higher, the greater amount of charges will cause the jet to accelerate faster and more volume of solution will be drawn from the tip of the needle. This may result in a smaller and less stable Taylor Cone. When the drawing of the solution to the collection plate is faster than the supply from the source, the Taylor Cone may recede into the needle [8].

The SEM images of the electrospun nylon 6 nanofibers in Figure 5 revealed that the dominant diameters of the nanofiber produced at 5 kV (Figure 5a) are in the range of 51 to 60 nm, which is considered very good range of diameters but the yield of nanofibers was very low. By increasing the applied voltage to 7 kV (Figure 5b), the fiber diameter is increased in the range from 60 to 80 nm and the yield was also low. Further increase in the voltage to 10 kV, the dominant diameter is increased in a range varied from 101 to 110 nm as shown in Figure 5c. At 15 kV (Figure 5d), the produced nanofibers are in the range of 40 to 50 nm. Finally, at 20 kV the dominant diameters are in the range of 101 to 110 nm (Figure 5e). By comparing the nanofibers diameters range produced from all previous power supply DC voltage, the optimum diameters range is produced from 15 kV.

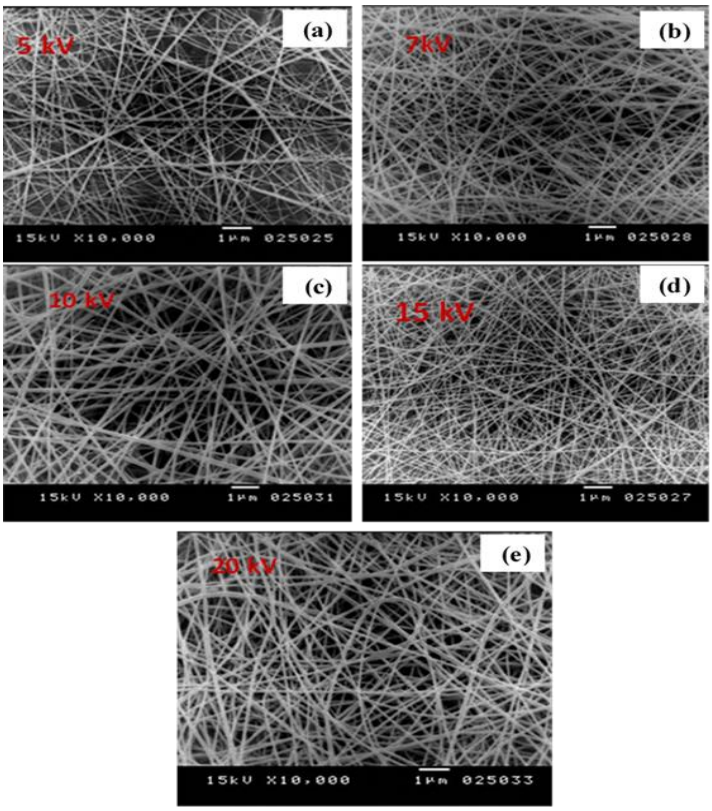

Figure 5. SEM images of nylon 6 nanofiber at concentration of 30 wt % and applied different voltages.

Journal of Climate Change Action, 2024, Vol. X, Iss. X, 1-11
DOI: 10.62184/jcca.jccaj100020241

Research Article

3.2.3. Effect of the flow rate

From the morphological analysis of electrospun nylon 6 nanofiber using 30 wt % solutions at different pump flow rate shown in Figure 6, a flow rate of 0.5 ml/hr is chosen as an optimum rate due to the formation of a stable Taylor cone, less instabilities and the narrowest fiber diameter distribution throughout the process (Figure 6 b). However, at flow rates below and above the threshold value, the asymmetric Taylor cone becomes less stable which produced wider nanofiber diameters distributions. At this flow rate, the feeding rate is proportional to the electrospinning speed. In this case, the electrospinning process is accomplished under a stable condition a lesser probability of instability and lesser falling droplets of the unspun polymer jet which allows sufficient time for evaporating the residual solvent and producing uniform fibers [28].

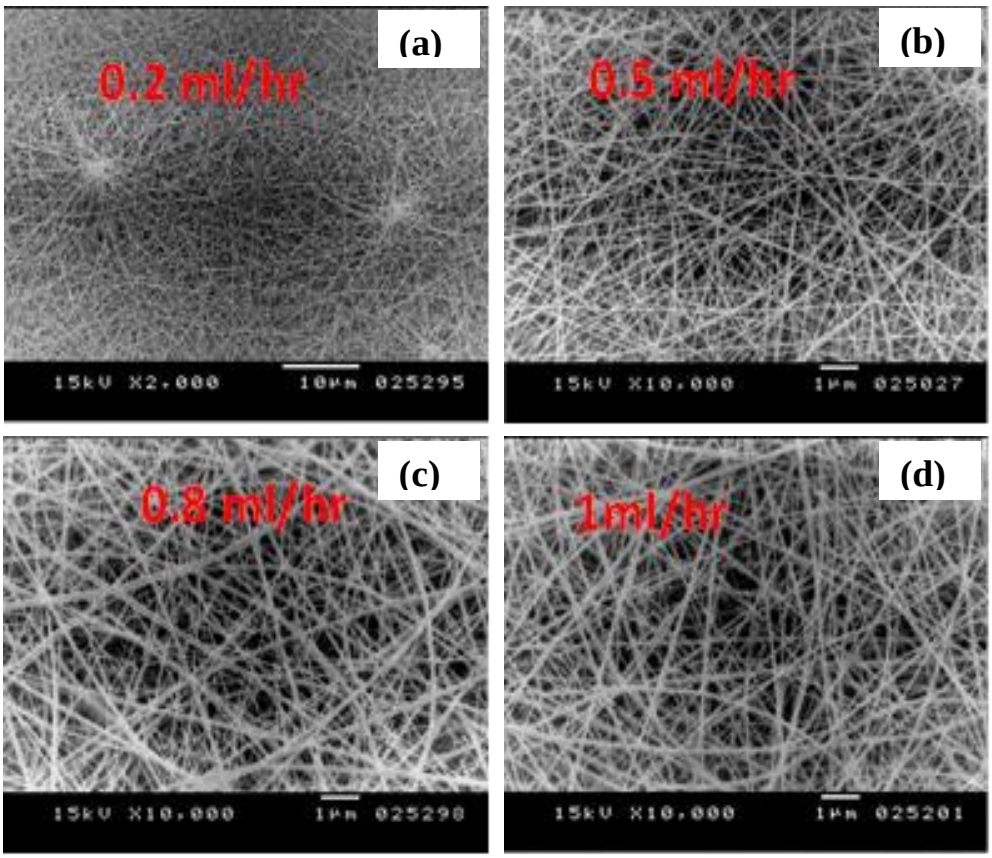

Figure 6. SEM images of electrospun nylon 6 nanofiber using 30 wt % solutions at different pump flow rates.

3.3. Contact angle measurements

The wettability behavior of the nylon 6 nanofiber is observed as 61º which refers to the nanofibers is slightly hydrophilic. It is noted that the water drop wasn't adsorbed immediately onto the nanofibers as shown in Figure 7a, while the nanofiber is oleophilic where the adsorption of motor oil by nanofibers occurred instantly so there is no ability to measure the contact angle between oil and nanofibers. There is no constant drop of motor oil on the nanofibers as shown in Figure 7b.

DOI: 10.62184/jcca.jccaj100020241

Research Article

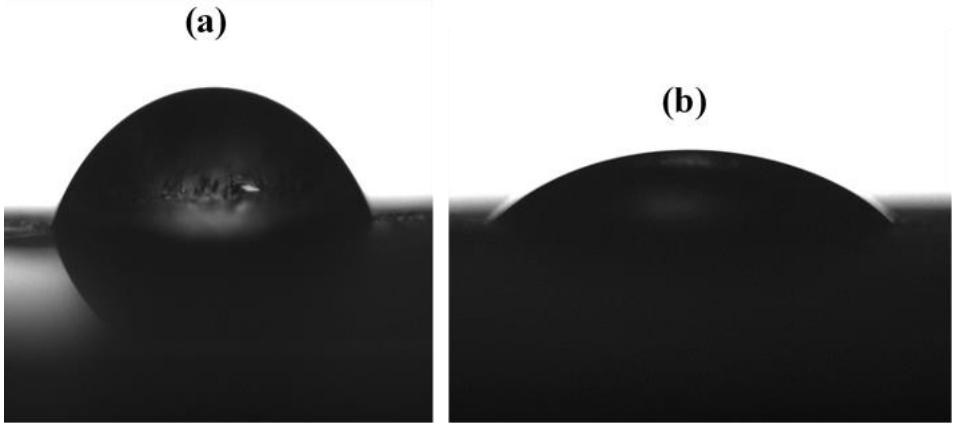

Figure 7. Wettability analysis of the electrospun nanofiber: Optical images of (a) a water droplet and (b) an oil droplet on the surface of the nanofiber.

3.4. Sorption of motor oil using nylon 6 nanofibers from electrospraying and electrospinning

Prior to the sorption experiments, the performance of nylon 6 nanofibers prepared from two concentrations of nylon 6/ formic acid (10 and 30 wt %) at 15 kV with flow rate of 0.5 ml/hr and distance of 15 cm between tip and collector for motor oil are investigated. It is observed that there is no adsorption of the oil on the surface of the nanofibers prepared from the concentration of 10 wt%. This is due to these fibers having a large number of beads "electrospray". Contrastingly, the nanofibers made from 30 wt% showed adsorption of the oil due to the small diameter of the nanofibers (40 to 60 nm) which led to high surface area and its oleophilic properties (high affinity to oil). The estimated oil sorption capacity for 55.9 mg of dry nylon 6 nanofibers using equation (1) is 18.2 g/g (the weight of this nanofiber after oil adsorption is 1073.6 mg). Consequently, these nanofibers adsorb oil 19.2 times its dry weight.

3.4.1. Effect of immersion time on oil sorption performance

Under the condition of the mass of 25 mg of nylon 6 nanofibers prepared from a solution of 30 wt% nylon 6/ formic acid at 15 kV with a flow rate of 0.5 ml/hr, different immersion times varied from 0.5 to 30 min are selected to investigate the relationship between the immersion time with the oil sorption capacity. As shown in Figure 8, the sorption capacity increases from 59 to 85 g/g with increasing the contact time from 0.5 to 30 min.

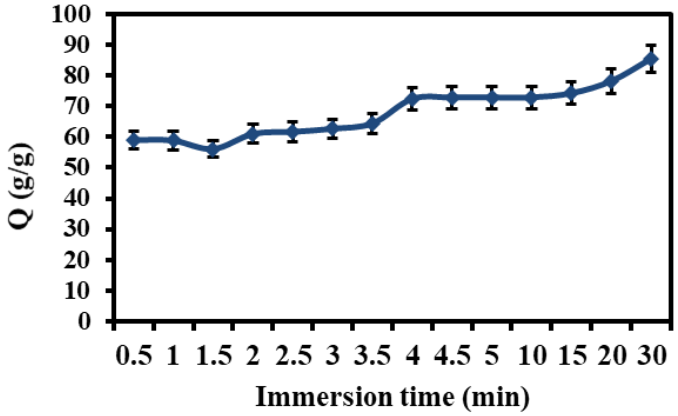

Figure 8. Q vs. immersion time for the removal of motor oil using 25 mg of nylon 6 nanofibers.

DOI: 10.62184/jcca.jccaj100020241

Research Article

4. Conclusion

In this work, electrospun nylon 6 nanofibers were successfully prepared from nylon 6 polymer using different concentrations of nylon 6 / formic acid solutions for the adsorption of motor oil. The optimal preparation conditions were obtained by exploring the effects of the concentration of nylon 6/ formic acid solutions, the applied voltage, the flow rate on the oil sorption capacity. The physicochemical properties of nylon 6 nanofibers were determined using FTIR, XRD, SEM and contact angle measurements. Compared to nylon 6 nanofibers prepared from 10 wt% nylon 6 /formic acid, the nanofibers of 30 wt% concentration has better performance in adsorption capacity. The sorption capacity increased with time and achieved a higher value of 85.38 g/g in a short time of 30 min for 10 mL of motor oil.

Author Information

Corresponding Author: Azza Shokry*

E-mail: azzashokry@alexu.edu.eg

ORCID iD: 0000-0001-6625-2874

Credit author statement

Faten Riad: Conceptualization, Data curation, Formal analysis, Investigation, Methodology, Writing - original draft. **Hesham Ibrahim**: Conceptualization - Supervision - Review & Editing. **Moataz Soliman**: Supervision - Review & Editing. **Shaker Ebrahim**: Conceptualization, Supervision, Data curation, Formal analysis, Review & Editing. **Azza Shokry**: Conceptualization, Supervision, Data curation, Formal analysis, Review & Editing.

Declaration of competing interest

The authors declare that they have no known competing financial interests or personal relationships that could have appeared to influence the work reported in this paper.

Data availability

Data will be made available on request

References

[1] Pintor, A. M. A., Vilar, V. J. P., Botelho, C. M. S., and Boaventura, R. A. R., (2016). Oil and grease removal from wastewaters: sorption treatment as an alternative to state-of-the-art technologies. A critical review. Chem. Eng. J., 297, 229. doi.org/10.1016/j.cej.2016.03.121.

[2] Kleindienst, S., Seidel, M., Ziervogel, K., Grim, S., Loftis, K., Harrison, S., Malkin, S. Y., Perkins, M. J., Field, J., Sogin, M. L., Dittmar, T., Passow, U. , Medeiros, P.M., and Joye, S. B., (2015). Chemical dispersants can suppress the activity of natural oil-degrading microorganisms. Proc. Natl. Acad. Sci. U.S.A., 112, 48, 14900. doi.org/10.1073/pnas.1507380112.

[3] Gupta, S., and Tai, N. H., (2016). Carbon materials as oil sorbents: A review on the synthesis and performance. J. Mater. Chem. A . 4, 1550. doi.org/10.1039/c5ta08321d.

[4] Kinner, N. E., Belden, L., and Kinner, P., (2014). Unexpected sink for deepwater horizon oil may influence future spill response. Earth Space Sci., 95, 21,176.

[5] Hubbe, M. A., Rojas, O. J., Fingas, M., and Gupta, B. S., (2013). Cellulosic substrates for removal of pollutants from aqueous systems: A review. 3. Spilled oil and emulsified organic liquids. J. Bioresour., 8, 2, 3038. doi.org/10.15376/biores.8.2.3038-3097.

[6] Prendergast, D. P., and Gschwend, Ph. M., (2014). Assessing the performance and cost of oil spill remediation technologies. J. Clean. Prod., 78, 233. doi.org/10.1016/j.jclepro.2014.04.054.

[7] Wen, Z., Wang, S., Bao, Z., Shi, S., and Hou, W., (2020). Preparation and oil absorption performance of polyacrylonitrile fiber oil absorption material. Water Air Soil Pollut., 231, 153. doi.org/10.1007/s11270-020-04524-y.

[8] Andrady, A., L., (2008). Science and technology of polymer

DOI: 10.62184/jcca.jccaj100020241

Research Article

nanofibers. ISBN 978-0-471-79059-4, John Wiley & Sons, Inc., Hoboken, New Jersey. doi.org/10.1002/macp.201000211.

[9] Moura, F. C. C., Lago, and R. M., (2009). Catalytic growth of carbon nanotubes and nanofibers on vermiculite to produce floatable hydrophobic 'nanosponges' for oil spill remediation. Appl. Catal., B., 90 (3–4), 436. doi.org/10.1016/j.apcatb.2009.04.003.

[10] Liang, H. W., Guan, Q. F., Chen, L. F., Zhu, Z., Zhang, W. J., and Yu, S. H., (2012). Macroscopic-scale template synthesis of robust carbonaceous nanofiber hydrogels and aerogels and their applications. Angew. Chem., 124, 21, 5191. doi.org/10.1002/anie.201200710.

[11] Sarbatly, R., Krishnaiah, D., and Kamin, Z., (2016). A review of polymer nanofibres by electrospinning and their application in oil–water separation for cleaning up marine oil spills. Mar. Pollut. Bull., 106,1–2, 8. doi.org/10.1016/j.marpolbul.2016.03.037.

[12] Martin, C.R., (1995). Template synthesis of electronically conductive polymer nanostructures. Acc. Chem. Res., 28, 2, 61. doi.org/10.1021/ar00050a002.

[13] van de Witte, P., Dijkstra, P.J., van den Berg, J.W.A., and Feijen, J., (1996). Phase separation processes in polymer solutions in relation to membrane formation. J. Membr. Sci., 117, 1. doi.org/10.1016/0376-7388(96)00088-9.

[14] Harfenist, S. A., Cambron, S. D., Nelson, E. W., Berry, S. M., Isham, A. W., Crain, M. M., Keynton, R. S., and Cohn, R. W., (2004). Direct drawing of suspended filamentary micro-and nanostructures from liquid polymers. Nano Lett. 4 (10), 1931. doi.org/10.1021/nl048919u.

[15] Khalaf, D. M., Elkatlawy, S. M., Sakr, A. A., and Ebrahim, S. M., (2020). Enhanced oil/water separation via electrospunpoly(acrylonitrile-co-vinyl acetate)/single-wall carbonnanotubes fibrous nanocomposite membrane. J. Appl. Polym. Sci., 49033. doi.org/10.1002/app.49033.

[16] Huang, Z. M., Zhang, Y. Z., Kotaki, M., and Ramakrishna, S., (2003). A review on polymer nanofibers by electrospinning and their applications in nanocomposites. Compos. Sci. Technol., 63, 15, 2223. doi.org/10.1016/S0266-3538(03)00178-7.

[17] Venugopal, J. and Ramakrishna, S., (2005). Applications of polymer nanofibers in biomedicine and biotechnology. Appl. Biochem. Biotechnol., 125, 147157. doi: 10.1385/abab:125:3:147.

[18] Hassan, A. M., Fadl, E. A., and Ebrahim, S. (2020). Electrospinning of polystyrene polybutadiene copolymer for oil spill removal. SN Appl. Sci., 2, 334. doi.org/10.1007/s42452-020-2118-4.

[19] Alnaqbi, M. A., Greish,Y. E., Mohsin, M. A., Elumalai, E. J. and Al Blooshi. A. (2016). Morphological variations of micro-nanofibrous sorbents prepared by electrospinning and their effects on the sorption of crude oil. J. Environ. Chem. Eng. , 4(2), 1850. doi.org/10.1016/j.jece.2016.02.030.

[20] Lin, J., Shang, Y., Ding, B., Yang, J., Yu, J. and Al-Deyab, S. S. (2012). Nanoporous polystyrene fibers for oil spill cleanup. Mar. Pollut. Bull. , 64(2), 347. doi.org/10.1016/j.marpolbul.2011.11.002.

[21] Mahdi, H. A. (2011). An FTIR study of characterization of neat and UV stabilized nylon 6,6 polymer films. Ibn al-Haitham j. pure appl. sci., 24(1), 86.

[22] Kimura, N., Kim, H. K., Kim, B. S., Lee, K. H. and Kim, I. S. (2010). Molecular orientation and crystalline structure of aligned electrospun Nylon-6 nanofibers: Effect of gap size. Macromol. Mater. Eng., 295(12),1090. doi.org/10.1002/mame.201000235.

[23] Pardo, F. N., Rivera-lópez, A., Sánchez-labastida, V. and Martínez, A. (2014). Statistical study of process parameters effect on crystallinity of electrospun polyamide 6, 6 Fibres. ECM, 1. doi.org/10.3390/ecm-1-c007.

[24] Kołbuk, D., Sajkiewicz, P., Maniura-Weber, K. and Fortunato, G. (2013). Structure and morphology of electrospun polycaprolactone/gelatine nanofibres. Eur. Polym. J., 49(8), 2052. doi.org/10.1016/j.eurpolymj.2013.04.036.

DOI: 10.62184/jcca.jccaj100020241

Research Article

[25] Liu, Y., Cui, L., Guan, F., Gao, Y., Hedin, N. E., Zhu, L. and Fong, H. (2007). Crystalline morphology and polymorphic phase transitions in electrospun Nylon-6 nanofibers. Macromol., 40(17), 6283. doi.org/10.1021/ma070039p.

[26] Ramakrishna, S., Fujihara, K., Teo, W. E., Lim, T. Ch. & Ma, Z. (2005), An introduction to electrospinning and nanofibers, World Scientific Publishing Co. Pte. Ltd, Singapore. doi.org/10.1142/5894.

[27] Bock, N., Woodruff, M. A., Hutmacher, D. W. and Dargaville, T. R. (2011). Electrospraying, a reproducible method for production of polymeric microspheres for biomedical applications. Polymers, 3(1),131. doi.org/10.3390/polym3010131.

[28] Zargham, Sh., Bazgir, S., Tavakoli, A., Rashidi, A. S. and Damerchely, R. (2012). The effect of flow rate on morphology and deposition area of electrospun Nylon 6 nanofiber. J. Eng. Fibers Fabr., 7(4), 155892501200700. doi.org/10.1177/155892501200700414.

[29] Riris, S., Bertolomeus, H. A. , Yadi, M. R., Maria, G. S. , William, X. W. , Dian, A. H., Dhewa, E., and Khairurrija, Kh. (2024). Optimization of electrospinning process parameters using Box-Behnken design for Nylon-6 nanofibers fabrication. Mater. Today Proc.. In press. doi.org/10.1016/j.matpr.2024.03.009.

[30] Liyuan, Z., Qiumeng, Z., Xinchang, Ge, Hongyu, Ch., Guoqing, Z., Kuanjun, F., andYueyao, L. (2023). Preparation of Nylon-6 micro-nanofiber composite membranes with 3D uniform gradient structure for high-efficiency air filtration of ultrafine particles. Sep. Purif. Technol., 308, 122921. doi.org/10.1016/j.seppur.2022.122921.

[31] Prasanta, K. P., Archana, G., and Amol, G. Th. (2022). Optimization of Nylon 6 electrospun nanofiber diameter in needle-less wire electrode using central composite design and response surface methodology. J. Ind. Text., 51(5S), 7279S. doi/pdf/10.1177/15280837211058213.

[32] NJR, B., TRA, B., and Roshan, P. (2024) Electrospinning drafting system for polyamide 6 and polyamide 6.6 nanofiber production. J. Text. Res. , 94(3–4), 341. doi.org/10.1177/00405175231205320.